RESEARCH ARTICLE | FEBRUARY 22 2007

Vibrational dynamics and stability of the high-pressure chain and ring phases in S and Se

Olga Degtyareva; Eduardo R. Hernández; Jorge Serrano; Maddury Somayazulu; Ho-kwang Mao; Eugene Gregoryanz; Russell J. Hemley

J. Chem. Phys. 126, 084503 (2007)
https://doi.org/10.1063/1.2433944

Vibrational dynamics and stability of the high-pressure chain and ring phases in S and Se

Olga Degtyareva
Geophysical Laboratory, Carnegie Institution of Washington, Washington DC 20015 and Centre for Science at Extreme Conditions, School of Physics, University of Edinburgh, Mayfield Road, Edinburgh EH9 3JZ, United Kingdom

Eduardo R. Hernández
Institut de Ciencia de Materials de Barcelona, CSIC, Campus de Bellaterra, 08193 Barcelona, Spain

Jorge Serrano
European Synchrotron Radiation Facility, Boîte Postal 220, 38043 Grenoble, France

Maddury Somayazulu and Ho-kwang Mao
Geophysical Laboratory, Carnegie Institution of Washington, Washington DC 20015

Eugene Gregoryanz
Geophysical Laboratory, Carnegie Institution of Washington, Washington DC 20015 and Centre for Science at Extreme Conditions, School of Physics, University of Edinburgh, Mayfield Road, Edinburgh EH9 3JZ, United Kingdom

Russell J. Hemley
Geophysical Laboratory, Carnegie Institution of Washington, Washington DC 20015

(Received 17 October 2006; accepted 20 December 2006; published online 22 February 2007)

The high-pressure phases of group-VI elements sulfur and selenium in their spiral chain and ring structures are examined by *in situ* Raman and x-ray diffraction techniques combined with first principles electronic structure calculations. The S-II, S-III, Se-I, and Se-VII having spiral chain structures and S-VI with a molecular six-member ring structure are studied in a wide *P-T* range. The square spiral chain structure of S-III and Se-VII is characterized by seven Raman modes that harden with increasing pressure. The calculations reproduce the observed frequencies and allow the authors to make the mode assignment. The "p-S" and "hplt" phases of sulfur reported by previous Raman studies are identified as S-II and S-III with the triangular and square spiral chain structures, respectively. The phase relations obtained by the x-ray and Raman measurements show that the high-pressure high-temperature phases of sulfur, observed by x-ray, can be induced by laser illumination at room temperature. © *2007 American Institute of Physics*. [DOI: 10.1063/1.2433944]

I. INTRODUCTION

Sulfur exhibits rich polymorphism under pressure, with the formation of numerous stable and metastable phases. Recent *in situ* x-ray diffraction studies have provided clarification of the formation conditions of several high-pressure phases of sulfur, and have given details of their crystal structures[1–4] (Fig. 1). The most common sulfur polymorph at ambient pressure, the orthorhombic S-I phase with eight-member ring molecules (S_8) transforms to the S-II phase above 1.5 GPa when heated close to the melting temperature.[1,3] S-II is shown to have a trigonal structure consisting of spiral chains with a triangular geometry.[1] The spiral chains of S-II have the same geometry as those found in trigonal Se-I, but within a larger unit cell. If S-II quenched to room temperature is pressurized above 36 GPa, it transforms to S-III, with a negative *P-T* transition slope.[3] The S-III phase has a tetragonal structure consisting of spiral chains with a square geometry.[2,3] This structure type is not unique to sulfur; it also forms at high pressures in orthorhombic Se (Ref. 2) and at high pressures and high temperatures in trigonal Se (in the Se-VII phase).[3] S-III has been shown to be stable up to 83 GPa, where it transforms to the metallic S-IV phase with an incommensurately modulated structure,[5,6] which then transforms to S-V with a β-Po structure at 153 GPa.[6,7] Evidence for a phase appearing between S-III and S-IV with a triclinic symmetry has been obtained.[5]

Heating of the S-II phase at 7–11 GPa above 650 K results in a transformation to another phase, labeled here as S-VI. This phase has been shown by *in situ* x-ray diffraction to have a rhombohedral structure and consists of six-membered ring molecules (S_6) (Ref. 4) (Fig. 1). The structure of S-VI is analogous to the ambient-pressure rhombohedral polymorph of S and Se that consists of S_6 or Se_6 molecules. Earlier we reported the observation of a phase other than II and III if sulfur was heated to 850 K at 5–15 GPa on decreasing pressure.[3] A comparison of our diffraction patterns[3] with those reported in Ref. 4 shows that the observed transformation at 9 GPa and 780 K corresponds to the transition from S-III into a mixture of S-II and S-VI.

The S-II phase can be quenched to room temperature and is observed over a large pressure range from ~3 to 36 GPa at 300 K.[3] The S-III and Se-VII phases hav-

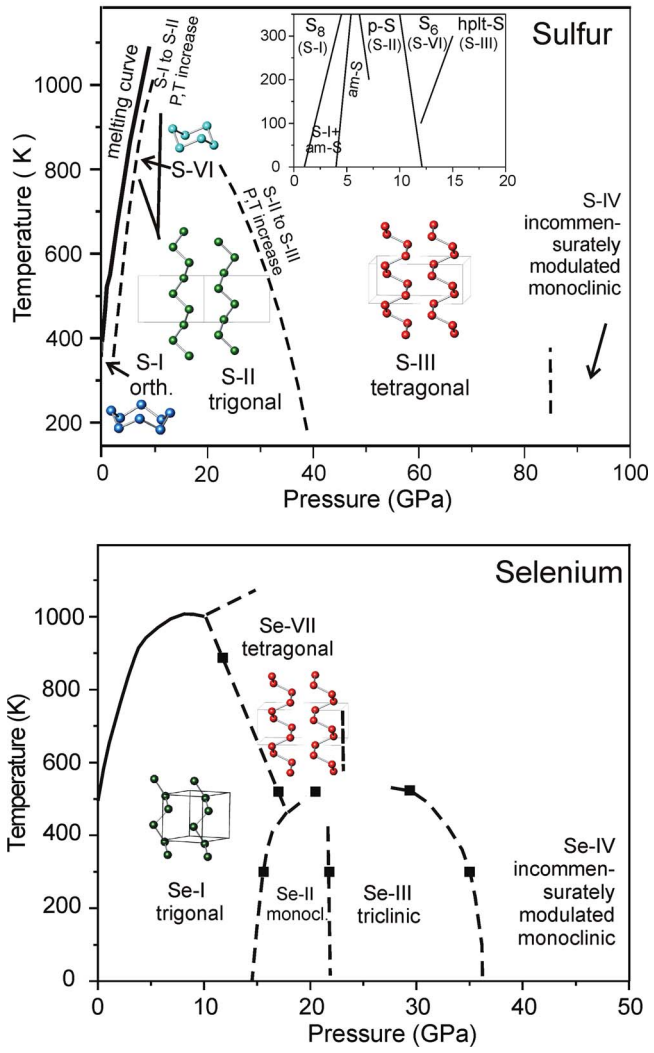

FIG. 1. (Color online) (Upper) Reaction and transformation diagram of sulfur obtained from x-ray data (modified from Ref. 3). The boundaries for the transitions S-I to S-II and S-II to S-III observed in Ref. 3 are shown by dashed lines. Stability region of the S-VI (S_6) phase is shown as reported in Ref. 4. Inset shows the *P-T* phase diagram of sulfur obtained from Raman spectroscopic studies (modified from Ref. 16). (Lower) Phase diagram of selenium with symbols indicating observed phase transitions (Refs. 37–39) and dashed lines showing tentative phase boundaries.

ing the same tetragonal spiral chain structure are also quenchable to room temperature, and after quenching are observed in a large pressure range from ~3 GPa in S (ambient pressure in Se) up to the pressure of transformation to the S-IV/Se-IV phases.[3] The large pressure range in which these quenched phases are observed and the irreversibility of the transitions at room temperature leave open the question about their true stability ranges. Compression of S-I at room temperature does not result in a transformation until the pressure of 36 GPa is reached, at which point it finally transforms to tetragonal S-III,[3] thus bypassing the transitions to S-II and S-VI.

There have been numerous *in situ* Raman measurements on various high-pressure phases of sulfur.[8–16] The results are dependent on laser energy and laser power density, and are therefore different from those reported from x-ray diffraction (Fig. 1, inset). A transformation from the ambient-pressure phase consisting of S_8 molecules to a photosensitive chain-like "p-S" phase has been reported at 3–10 GPa.[9–16] The S_8 (S-I) phase transforms to p-S via an intermediate amorphous a-S phase, which occurs at 5–12 GPa.[12,14–16] A transformation from the p-S phase to the six-member ring molecular sulfur S_6 is reported at pressures of about 9–13 GPa.[8,10,12–16] Another phase, called high-pressure low-temperature ("hplt") sulfur, is observed to form at about 12–14 GPa if low laser power density is used.[8,12]

It has been noted previously that sulfur is sensitive to laser light and can undergo laser-induced structural transformations under pressure (see, for example, Refs. 11 and 16). The laser-induced high-pressure transitions in sulfur measured by Raman spectroscopy have thus not been confirmed by other (room-temperature) measurements, including x-ray diffraction, differential thermal analysis, and optical absorption. Indeed, room-temperature x-ray diffraction measurements[2,3,5,6,11] show no evidence for the phase transitions in the pressure region in which Raman studies found numerous transformations (3–14 GPa). Infrared spectroscopy[17] is consistent with the lack of phase transitions up to 10 GPa found by x-ray diffraction. These discrepancies between different techniques have led to confusion about the *P-T* phase diagram of sulfur. We address some of these questions in the present work.

Although the structural and vibrational properties of the S_6 phase (S-VI) are fully characterized by *in situ* x-ray diffraction and Raman spectroscopy,[4,8] the nature of the p-S and hplt sulfur phases has not been fully clarified. Recent reports of novel spiral chain structures in sulfur and the heavier group-VI element Se (Refs. 2 and 3) require the complementary characterization of their vibrational properties. In this paper we report the results of a combined experimental and theoretical study of the vibrational dynamics of the high-pressure phases in sulfur and selenium, employing Raman and x-ray techniques as well as first principles electronic structure calculations. We identify the p-S and hplt sulfur phases as spiral chain structures with triangular and square geometries and compare them with the well-characterized S_6 phase.

The structure of this paper is as follows: in Sec. II we provide a brief description of the experimental and computational techniques employed in this study; in Sec. III we discuss the experimental results and provide a comparison with predictions from first principles calculations for each of the phases considered in this work, and we also review the consequences of these results on the phase diagram of sulfur. Finally, our conclusions are summarized in Sec. IV.

II. METHODS

A. Experiment

The experiments were performed on polycrystalline samples of S and Se (99.999% purity) loaded in Mao-Bell piston-cylinder diamond anvil cells (DACs). Powder diffraction data were collected at beamline 16-ID-B (HPCAT) at the Advanced Photon Source. A focused, monochromatic beam (wavelengths in the range $\lambda = 0.36–0.42$ Å) was used, and data were recorded on an image plate calibrated with CeO_2 or Si standard. X-ray diffraction data were collected *in situ* at

TABLE I. Structural data on some high-pressure phases of sulfur and selenium.

Phase	P,T	Space group	Lattice parameter	Atomic positions	Ref.
S-II	3 GPa	$P3_221$	7.0897	$6c$ (0.773,0.307,0.611)	1
	573 K	No. 154	4.3024	$3b$ (0.876,0,1/6)	
S-II	5.8 GPa	$P3_221$	6.9082	$6c$ (0.230,0.543,0.051)	3
	800 K	No. 154	4.2593	$3b$ (0.876,0,1/6)	
S-VI	7.2 GPa	R-3	10.1508	$18f$	4
S_6	950 K	No. 148	3.6756	(0.1758,0.1925,0.1503)	
S-VI	6.5 GPa	R-3	10.165	$18f$	This
S_6	816 K	No. 148	3.687	Not refined	work
S-III	12 GPa	$I4_1/acd$	8.5939	$16f$ (0.141,0.141,1/4)	3
	300 K	No. 142	3.6179	(origin choice 1)	
S-III	42 GPa	$I4_1/acd$	8.054	$16f$ (0.131,0.131,1/4)	This
	300 K	No. 142	3.249	(origin choice 1)	work
S-III	55 GPa	$I4_1/acd$	7.841	$16f$ (0.136,0.136,1/4)	2
	300 K	No. 142	3.100	(origin choice 1)	
Se-VII	11.9 GPa	$I4_1/acd$	9.201	$16f$ (0.131,0.131,1/4)	This
	300 K	No. 142	3.680	(origin choice 1)	work
Se-VII	15.3 GPa	$I4_1/acd$	9.148	$16f$ (0.132,0.132,1/4)	2
(Se-II′)	300 K	No. 142	3.626	(origin choice 1)	
Se-VII	16.2 GPa	$I4_1/acd$	9.0753	$16f$ (0.129,0.129,1/4)	3
	300 K	No. 142	3.6206	(origin choice 1)	

room and at high temperatures in an externally heated DAC.

For the Raman spectroscopy measurements a custom-build high-pressure Raman setup at the Geophysical Laboratory was used.[18] Raman spectra were excited with the 488.0 and 514.5 nm lines of an Ar-ion laser with a laser power of about 50 mW and a laser focal spot of about 5 μm. All Raman spectra were measured at room temperature. The Raman spectra were analyzed by a single-stage spectrograph with a multichannel charge coupled device detector. No pressure transmitting medium was used. This ensured that the sample in direct contact with the culet of a diamond anvil formed a surface with high optical quality that improves the coupling of the laser beam with the material under pressure. The pressure was determined by the ruby fluorescence method.

The low laser power was used for Raman measurements to avoid heating of the sample and to prevent phase transitions during those measurements. The x-ray diffraction patterns measured prior and after laser illumination were identical.

B. Computation

First principles calculations of the phonon modes at the Γ point were performed in order to characterize the experimentally measured Raman frequencies, their associated atomic displacements, and their irreducible representations. The experimental lattice parameters at several pressures were used, and the atomic positions were relaxed by means of the conjugate gradient technique. The VASP code,[19] which is based on density functional theory,[20] was used to calculate the atomic forces on a minimal set of displaced atoms. These forces were then used as input for the PHONON code[21] to calculate the phonon frequencies by the so-called direct method. We employed the projector augmented wave[22] formalism as implemented in the VASP package.[23] For both S and Se we considered six-electrons in the valence (the $3s^2$ $3p^4$ in the case of S and the $4s^2$ $4p^4$ in the case of Se); the energy cutoffs employed were 280 and 211 eV for S and Se, respectively. A larger energy cutoff (380 eV) was necessary to converge the phonon frequencies in the case of the molecular structures S-II and S-VI. The k-point sampling was adjusted in each particular structure so as to obtain well-converged total energies and forces. The generalized gradient approximation as parametrized by Perdew *et al.*[24] was employed to account for the exchange-correlation energy of the electrons.

III. RESULTS AND DISCUSSION

A. S-II: Triangular spiral chains

The structure of S-II has been shown to be trigonal with spiral atomic chains of triangular geometry and to form at 3–8 GPa by heating to temperatures close to melting[1,3] (Fig. 1). The S-II phase can be quenched to room temperature and is observed over a wide pressure range (up to 36 GPa at 300 K on pressure increase).[3] Details of the pressure dependence of the S-II crystal structure are given in our earlier paper,[25] while Table I provides the structural data at two particular pressure points. A theoretical group analysis[26] of the S-II structure for the $6c$ and $3b$ sites of the $P3_221$ space group predicts 13 Raman active modes, three A_1 and six E modes for the $6c$ position, and one A_1 and three E modes for the $3b$ position.

A photosensitive chainlike p-S phase is reported from Raman spectroscopy to form in the same pressure range at room temperature.[9–16] The Raman spectrum of the p-S phase is characterized by 11–12 frequencies,[12,16] the strongest eight of which can be seen in Fig. 2 (inset). The pressure dependence of the frequencies in p-S has been studied in

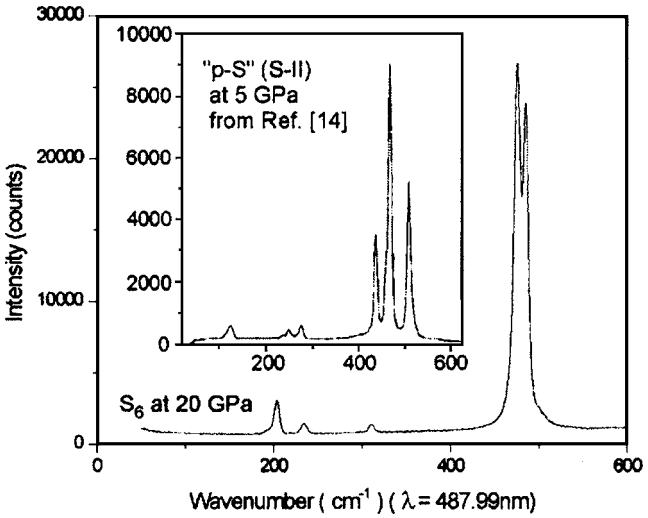

FIG. 2. Raman spectrum of the S-VI phase (S_6) obtained in present work at 20.0 GPa. The inset shows a Raman spectrum of the photosensitive sulfur p-S (S-II) at 5 GPa obtained by Orgzall and Lorenz (Ref. 14).

detail[12,13,16] and is shown in Fig. 3(a). The pressure range of appearance of the p-S phase (3–10 GPa at room temperature) reported from Raman studies is close to that of S-II, obtained from diffraction studies (3–8 GPa at high temperatures). Furthermore, the number of modes predicted for the S-II structure is close to that observed for the p-S phase. Thus, it appears that the S-II and p-S phases are the same or are closely related.

Indeed, our first principles calculations on S-II predict that, of the 13 Raman active modes allowed by symmetry considerations, one of the nine doubly degenerate modes of *E* character has zero frequency at 6 GPa, so we should expect to observe 12 modes (four A_1 and eight *E*) in the spectrum. The calculated frequency values for S-II (Table II) closely match those observed experimentally for the p-S phase, with a slight downward shift. Figure 4 illustrates the calculated Raman active modes for S-II at 6.0 GPa. Experimentally, only 11 modes are observed at this pressure,[15,16] and therefore it would seem as if there is one missing peak in the observed data, which could be due to an accidental (near) degeneracy between modes. As can be seen in Table II, two *E* modes are predicted to have fairly close frequencies (109 and 113 cm^{-1}), though these seem to correspond to the two modes experimentally observed at 130 and 132 cm^{-1}, respectively. Another case of closely matching frequencies is predicted to occur between different *E* modes at 428 and 432 cm^{-1}. Another possible explanation is that the missing mode is one of low intensity not resolved in the spectrum.

The modes with frequencies 150 cm^{-1} and below correspond to frustrated rotational or translational motions of the spiral S chains [Figs. 4(a)–4(d)]. Their displacements do not distort the chains. The modes with frequencies in the range of 200–300 cm^{-1}, all of them having an *E* character, induce bond-bending or torsional motions along the spiral chains, but there is little stretching of bonds [Figs. 4(e)–4(g)]. Finally, the modes with frequencies above 400 cm^{-1} are essentially bond-stretching modes [Figs. 4(h)–4(l)]. All modes in S-II display an increase in frequency as the pressure is

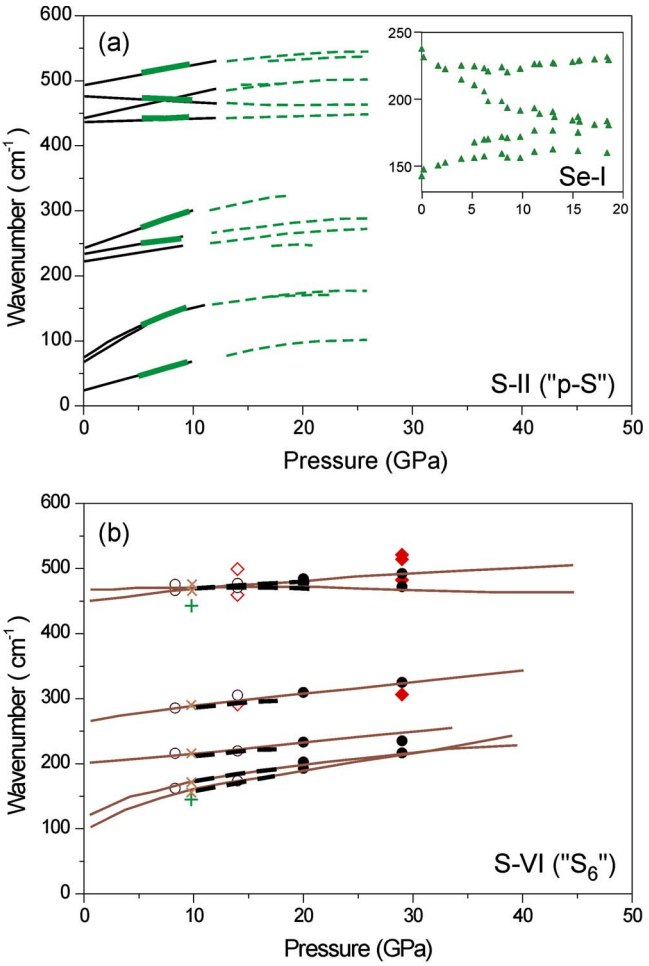

FIG. 3. (Color online) (a) Pressure dependence of the Raman modes for the S-II (p-S) phase with triangular chain structure. Thin solid lines show data from Ref. 16, thick solid lines - data from Ref. 13, and dashed lines - data from Ref. 12. The inset shows the pressure dependence of the Raman modes in Se-I, observed in the present work. (b) Pressure dependence of the Raman modes for the S-VI (S_6) phase. Solid lines show data from Ref. 8, dashed lines - from Ref. 13, crosses and pluses - from Ref. 10 with pluses showing the admixture of the S-II phase, and circles and diamonds - from present work with diamond showing the admixture of the S-III phase. Solid and open symbols denote data obtained on pressure increase and pressure decrease, respectively.

increased, with the exception of one (strongest) A_1 mode at 476 cm^{-1} (at ambient pressure), which corresponds to a symmetric stretching mode and shows a decrease in frequency with pressure increase. This softening of the strongest A_1 mode in S-II is also observed for the A_1 mode of Se and Te chain structures[27] (as shown in the inset to Fig. 3(a) for Se-I), and is explained by the idea of an increasing interaction between the chains with increasing pressure.

B. S-VI: S_6 rings

The S-VI phase has a rhombohedral structure composed of six-membered ring molecules[4] (Fig. 1). In our present x-ray diffraction study, the S-VI phase is observed to form at 7–11 GPa upon heating to 700–800 K, starting either from the S-II or S-III phases. Indexing of the S-VI patterns gave a rhombohedral cell with the space group $R\bar{3}$ and lattice parameters shown in Table I, confirming the solution reported

TABLE II. Observed and calculated Raman frequencies (cm^{-1}) and mode assignment for the S-II (p-S) phase of sulfur. s-stretching: b-bending. All experimental data refer to room temperature.

					b			s				
P (GPa)	A_1	A_1	E	E	E	E	E	E	E	A_1	A_1	Ref.
AP	27	71	85	96	224	237	249	437	444	476	496	15 and 16
6.0	51	125	130	132	239	253	279	437	476	470	512	15 and 16
6.0	34	107	109	113	227	239	263	404	428, 432	451	502	Calc. This work

in Ref. 4. We find that the S-VI phase is quenchable to room temperature and observable on pressure increase at least up to 30 GPa, and on pressure release down to 4 GPa. In the same pressure range at ambient temperature, the S-I, S-II (quenched from high temperatures), and S-III phases were observed,[3] thus leaving the question of the true P-T stability regions of these phases open. The experimental determination of the true stability range of S-VI (S_6) in the pressure range of 7–11 GPa and the temperature range of 650–1000 K has been claimed in Ref. 4. The pressure dependence of the structural parameters for the S-VI phase at 4–30 GPa measured in the present work is shown in Fig. 5. The measured values of the atomic volume of S-VI lie between the values of atomic volume determined for S-II and S-III (Ref. 3) (Fig. 5).

The group theory analysis[26] of the S-VI structure based on the 18f position of the $R\bar{3}$ space group predicts six Raman active modes, three A_g, and three E_g. The Raman spectrum of the S-VI phase obtained experimentally at room temperature and pressures of 9–13 GPa is characterized by six frequencies (Fig. 2, Table III), and is the same as previously reported for the S_6 phase.[8,9] The mode assignment can be found, for example, in the work of Haefner *et al.*[8] and is shown in

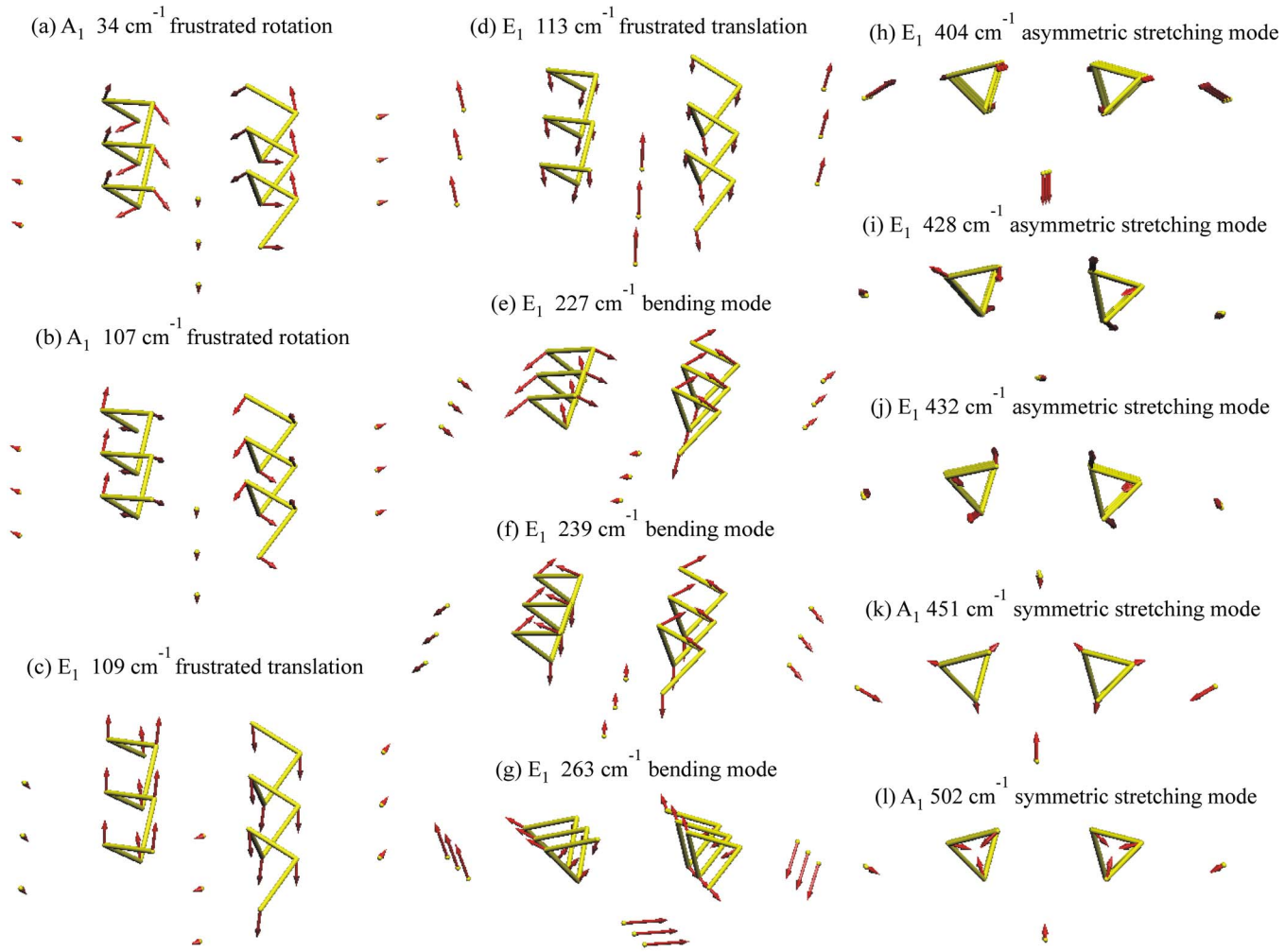

FIG. 4. (Color online) Raman active modes of the S-II phase with a triangular spiral chain structure, calculated for pressure of 6 GPa. Only one of the doubly degenerate E modes is shown in each case.

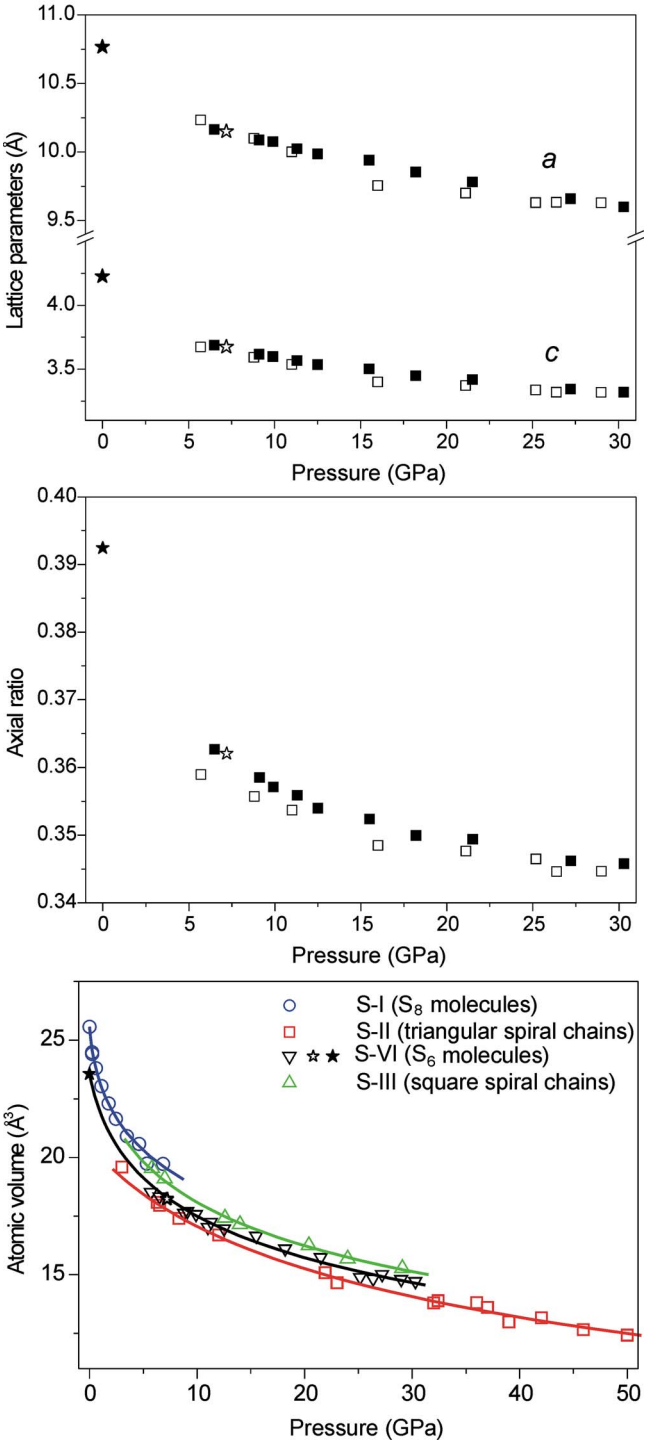

FIG. 5. (Color online) Pressure dependence of lattice parameters and axial ratio for the S-VI structure, determined in the present work. Solid and open symbols show the data collected on pressure increase and pressure decrease, respectively. The open star symbol shows the data from Ref. 4. Filled star symbol shows the data for the ambient-pressure metastable S_6 polymorph of sulfur from Ref. 40. The atomic volume of S-VI is shown in comparison with the volumes of the S-I, II, and III phases taken from our earlier work (Refs. 3 and 25).

Table III. The pressure dependence of the Raman frequencies of the S-VI (S_6) phase from the literature data is compared with data from the present work in Fig. 3(b). We compare our data with those of Haefner *et al.*[8] obtained up to 40 GPa, one data point at 9.7 GPa from Wolf *et al.*,[10] and the data in the pressure range of 10–18 GPa from Yoshioka and Nagata.[13] The Raman spectra for the S_6 phase in the pressure range of 2–11 GPa reported by Schumacher *et al.*,[28] at a pressure of 9.7 GPa by Orgzall and Lorenz,[14] and at 11.8 GPa and 20 K by Eckert *et al.*[15] agree with the data shown in Fig. 3(b).

We have calculated the Raman frequencies at a pressure of 7.3 GPa and have obtained values listed in Table III. Calculations resulted in six distinct frequencies, which are in reasonable agreement with the experimental values of Haefner *et al.*[8,9] obtained at 7.9 GPa. For the higher frequency modes, the agreement is better for the A_g modes, with a slight shift of 10–12 cm^{-1} to lower values with respect to the experimentally determined frequencies. This shift is at least partially due to the slightly lower pressure at which the calculations were performed. The E_g modes seem to be affected by a larger shift, ranging from 20 to 60 cm^{-1}. The vibrational modes of S-VI are shown in Fig. 6, including libration [(a) and (b)], bending [(c) and (d)] and stretching [(e) and (f)] modes.

A comparison with the assignment of the Raman active modes for the S_6 molecule made by Berkowitz *et al.*[29] and by Nimon *et al.*,[30] and with the more recent calculations of Wong *et al.*[31] confirms our assignment for the bending and stretching modes. These modes with frequencies from approximately 200 cm^{-1} upwards show a strongly molecular character and are practically indistinguishable from the corresponding modes in an isolated S_6 D_{3d} molecule, both in their frequencies and in the pattern of atomic displacements. Concerning the lower frequency modes (below 200 cm^{-1}), we obtain two frustrated rotational modes, one of which is a doubly degenerate E_g mode at 100 cm^{-1}, in which the molecules rigidly oscillate around a C_2 axis of the molecule and a nondegenerate A_{1g} mode at 141 cm^{-1}, in which the molecules attempt to rotate around the C_3 axis perpendicular to the plane of the molecules. These low energy modes are crystal modes which correspond to free rotations of the isolated molecule. This is in agreement with the assignment of librational modes made by Schumacher *et al.*[28] Their assignment also predicted that the A_{1g} mode would have a slightly higher frequency than the degenerate E_g mode, as confirmed by our calculations.

All six modes in S-VI harden with pressure. However, at pressures above 13 GPa, the strongest Raman mode at 470 cm^{-1} shows softening with pressure increase, while all other five modes continue to harden with pressure [Fig. 3(b)]. This soft mode corresponds to the symmetric S-S stretching mode A_1, similar to the 476 cm^{-1} symmetric stretching mode A_1 of S-II which is also soft [Fig. 3(a)].

C. S-III and Se-VII: Square spiral chains

The structure of S-III is tetragonal, consisting of spiral atomic chains with a square geometry, and is observed above 36 GPa at room temperature[2,3] (Fig. 1). The S-III phase is observed on pressure increase up to 86 GPa and on decompression to 3 GPa at room temperature.[3] The details on the pressure dependence of the S-III crystal structure in a wide pressure range of 3–74 GPa are given in our earlier paper,[25]

TABLE III. Observed and calculated Raman frequencies (cm^{-1}) and mode assignment for the S_6 phase of sulfur. All experimental data refer to room temperature. s-stretching, b-bending, lib-libration (hindered rotation), and AP-ambient pressure.

P,T	lib E_g	lib A_{1g}	b E_g	b A_{1g}	s E_g	s A_{1g}	Ref.
AP	95	120	203	267	452	470	8 and 9
7.9 GPa	156.3	171.4	215.9	288.2	468.5	474.9	8 and 9
8.3 GPa	···	162.2	216.1	285.8	466.3	475.7	This work Expt.
7.3 GPa	100.5	141	195	279	422	464	This work Calc.
20.0 GPa	193.1	202.7	233.3	309.6	484.3	474.9	This work Expt.

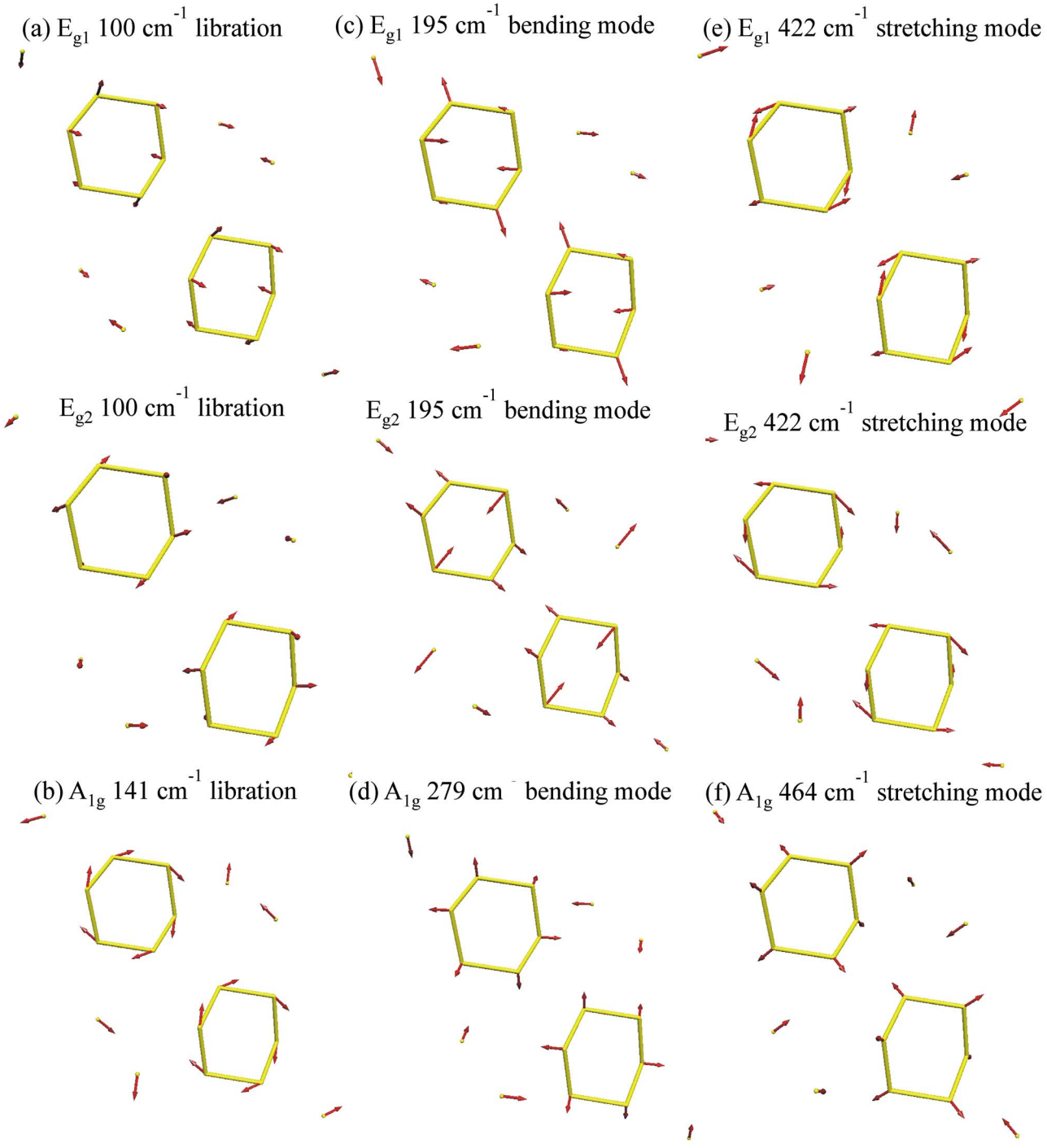

FIG. 6. (Color online) Raman active modes of the S-VI phase with the S_6 molecules, calculated for a pressure of 7 GPa.

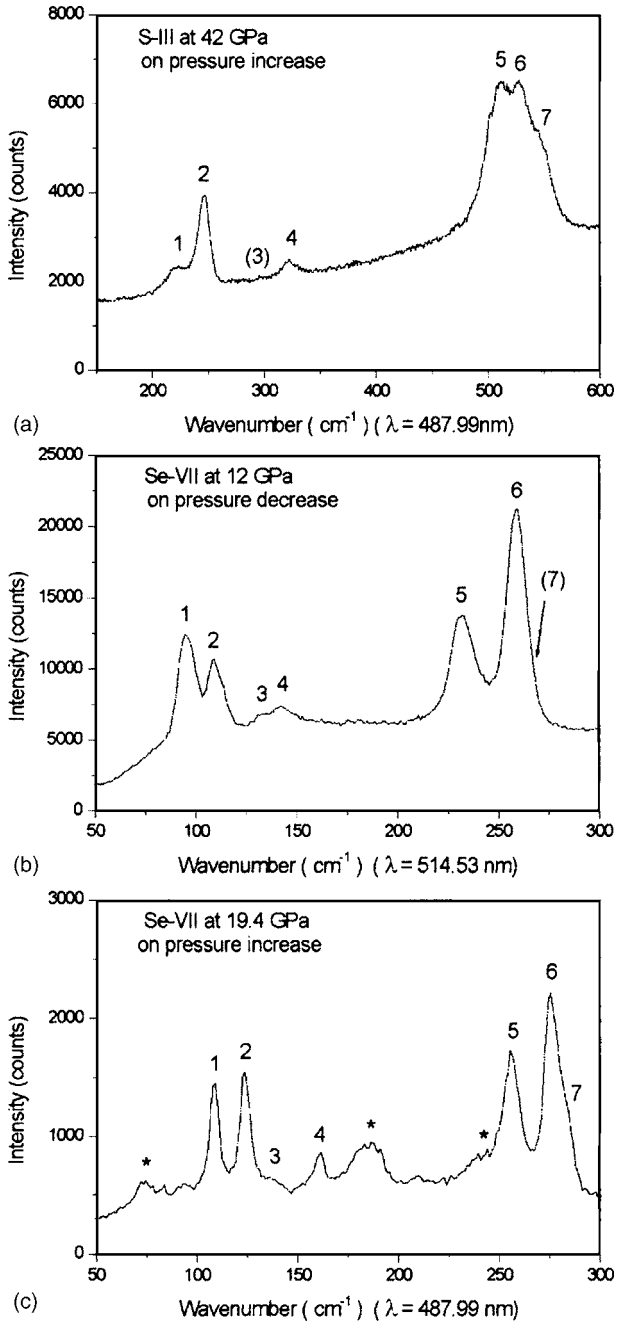

FIG. 7. Raman spectra of (a) S-III at 42 GPa, (b) Se-VII at 12 GPa, and (c) Se-VII at 19.4 GPa with a minor admixture of Se-IV (marked by asterisks).

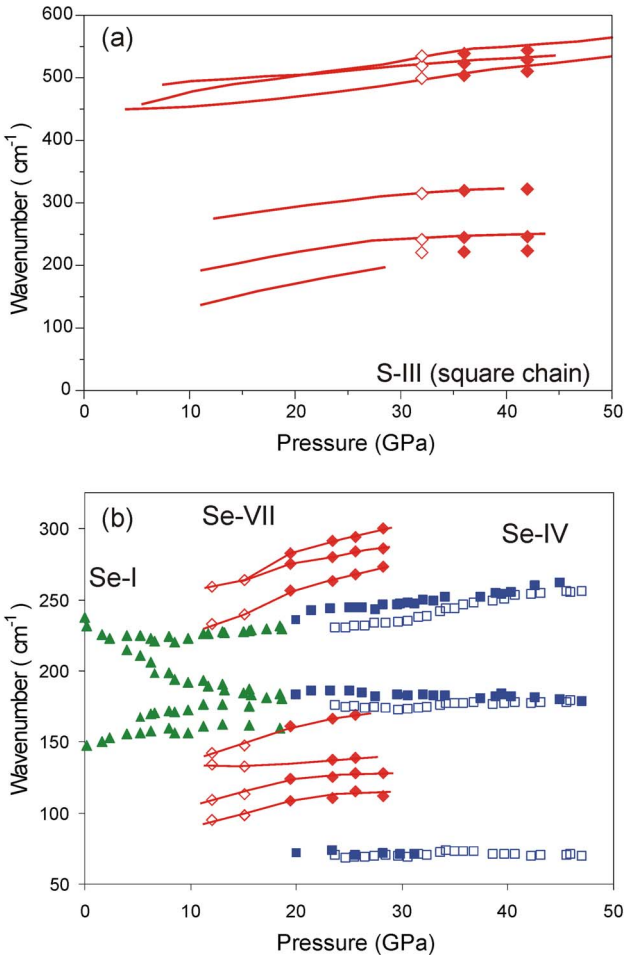

FIG. 8. (Color online) (a) Pressure dependence of the Raman frequencies for S-III: symbols-present work; lines-data from Refs. 8, 9, and 12. (b) Pressure dependence of the Raman frequencies for three Se phases from the present work: Se-I-triangles, Se-VII-diamonds, and Se-IV- squares. Lines are guides to the eye. Solid and open symbols denote data obtained on pressure increase and pressure decrease, respectively.

while Table I gives structural data for a few particular pressure points. The group theory analysis of the S-III structure based on placing sulfur atoms on the 16*f* site of the $I4_1/acd$ space group predicts seven Raman active modes, one A_{1g}, two B_{1g}, one B_{2g}, and three E_g modes. Our present Raman data for phase S-III give six strong Raman modes [Fig. 7(a)], all of them showing an increase with pressure [Fig. 8(a)].

The calculation of Raman modes for the S-III phase reveals the mode assignment for this structure (Table IV). The calculated frequency values show a satisfactory agreement with the observed values with a slight downward shift, in line with what is obtained for the other phases considered in this study. As shown in Fig. 9, the Raman active modes of the S-III structure having frequencies in the range of 200–300 cm^{-1} consist essentially of the distortion of bond angles along the square chains. The higher frequency modes in the range of 450–550 cm^{-1} are bond-stretching modes.

The S-III-type tetragonal structure with square spiral chains has also been reported at high pressures for both trigonal and orthorhombic modifications of Se.[2,3] Although orthorhombic Se transforms to Se-VII (Se-II′) at room temperature (at around 15 GPa),[2] trigonal Se requires high temperatures (of about 450 K at 20 GPa) for the transition to Se-VII.[3] We collected Raman data on the trigonal modification of Se at high pressure to characterize the vibrations of the square chain structure of Se-VII. The pressure dependence of the Raman modes for ambient-pressure Se-I [Fig. 8(b)] agrees with that reported in the literature for trigonal Se,[27] but also with the data for amorphous[32] and nanocrystalline[33] modifications of Se. Above 20 GPa, the three strong Raman modes are observed and assigned to the Se-IV phase, which has an incommensurately modulated structure.[34] The detailed analysis of the Raman data of Se-IV will be published elsewhere.

Using high incident laser power density and without ex-

TABLE IV. Observed and calculated Raman frequencies (cm^{-1}) and mode assignment for the square chain structure of S-III and Se-VII from present work. All experimental data refer to room temperature. s-stretching: b-bending.

Phase	P (GPa)	b B_{1g}	b E_g	b B_{2g}	b E_g	s A_{1g}	s E_g	s B_{1g}	
S-III	36.0	221.7	244.7	⋯	319.7	503.6	523.0	538.9	Expt.
S-III	36.8	197.8	216.0	276.4	295.3	467.1	479.5	482.8	Calc
Se-VII	12.0	95.0	109.2	131.5	142.0	232.8	258.7	⋯	Expt.
Se-VII	13.0	94.9	101.5	123.3	138.5	224.6	237.5	240.9	Calc.
Se-VII	19.4	108.4	123.6	⋯	161.0	255.7	274.6	279.5	Expt.
Se-VII	19.2	99.3	110.3	123.9	151.0	245.9	254.8	261.6	Calc.

ternal heating of the sample, we observe a transition from Se-II to a phase characterized by six to seven Raman modes [Figs. 7(b) and 7(c)]. These are very similar to the modes observed for S-III [Fig. 7(a)], with the frequencies having lower values. Thus, these observed modes are attributed to the tetragonal Se-VII phase. A summary of Raman modes for the square chain structures of S-III and Se-VII is given in Table IV. The calculation of the Raman active modes for the Se-VII phase confirms the mode assignment determined for S-III (Table IV). Similar to the S-III results, the calculated frequency values for Se-VII show a satisfactory agreement with the observed values with a slight downward shift.

As for S-III, all modes in Se-VII increase in frequency when pressure is increased [Fig. 8(b)], a trend which is reproduced in our calculations (Table IV). Interestingly, the Raman modes of Se-VII are mutually exclusive with those in Se-I and Se-IV [Fig. 8(b)], thereby amplifying the distinct difference between their crystal (and molecular) structures. In contrast, the Raman spectra for sulfur phases II, III, and VI are all rather similar.

Previous high-pressure Raman studies on sulfur, obtained with low laser power density that ensured that the sample was not heated, report the existence of another high-pressure phase of sulfur at pressures above 12–14 GPa.[8,9,12] This modification of sulfur was labeled as hplt phase and is characterized by five to six strong modes (see Fig. 8 in Ref. 12). The spectra are remarkably similar to those obtained in the present work for S-III. The pressure dependence of the Raman frequencies for the hplt phase is the same as in S-III [Fig. 8(a)]. It is thus clear that the hplt phase of sulfur[8,9,12] corresponds to the tetragonal S-III phase, although the hplt sulfur is observed by Raman spectroscopy at much lower pressures of 12 GPa, compared to the room-temperature x-ray diffraction observation of S-III above 36 GPa.

D. Phase relations in sulfur

Observation by x-ray diffraction of the phases S-II (p-S) and S-VI (S_6) requires heating to temperatures close to melting (Fig. 1). However, these phases are observed in sulfur by Raman spectroscopy at room temperatures, with transition pressures depending on the laser wavelength and laser power density.[11,15,16,35,36] The use of the blue and green laser light (energies of 2.54 and 2.41 eV, respectively) results in the lower transition pressures in comparison with the use of the yellow and red laser light (lower energies of 2.07 and 1.96 eV, respectively), which is connected with the decrease of the band gap in sulfur with pressure increase.[16] No transitions are observed up to 12 GPa by Raman spectroscopy if sulfur is illuminated with yellow and red laser light.[9,10,13,16] The room-temperature S-I to S-II transition observed by Raman studies has been suggested to occur due to the absorption of laser light by sulfur molecules which overcomes the activation energy necessary to break the S_8 molecules and thus facilitates polymerization.[16,35,36] As discussed recently,[4] the $S_8 \rightarrow$ polymeric $\rightarrow S_6$ sequence observed by Raman spectroscopy at room temperature[9,13] corresponds to the same sequence (S-I $\rightarrow$ S-II $\rightarrow$ S-VI) observed by x-ray diffraction at high temperatures, in the same pressure range (Fig. 1). Similarly, another polymeric S-III phase observed by diffraction above 36 GPa at room temperature,[2,3] or at high temperatures and lower pressures of 11 GPa,[3,4] corresponds to the same hplt phase of sulfur found in Raman studies at 10–15 GPa and room and low temperatures using low laser power density.[8,9]

All these observations indicate that the photoinduced phase transitions observed in Raman studies (Fig. 1 inset) correspond to the existing structural transitions in the phase diagram of sulfur determined by x-ray diffraction (Fig. 1). Laser illumination of sulfur in Raman measurements appears to play the same role as the external heating in the x-ray diffraction studies, inducing phase transitions by overcoming kinetic barriers associated with breaking down sulfur molecules.

IV. CONCLUSIONS

We have presented a detailed analysis of the vibrational properties of several phases of sulfur and selenium. In particular we have considered the polymeric structures S-II (trigonal) and S-III (tetragonal), together with Se-VII (isostructural with S-III), as well as the S_6 molecular S-VI phase. Raman spectra of the different phases have been obtained at varying pressures, and the frequencies of the different modes have been calculated for each structure employing first principles electronic structure calculations. This combined experimental-theoretical approach has allowed us to corroborate the mode assignment of previous studies and, in the case of S-II, S-III, and Se-VII, to obtain the mode assignment for

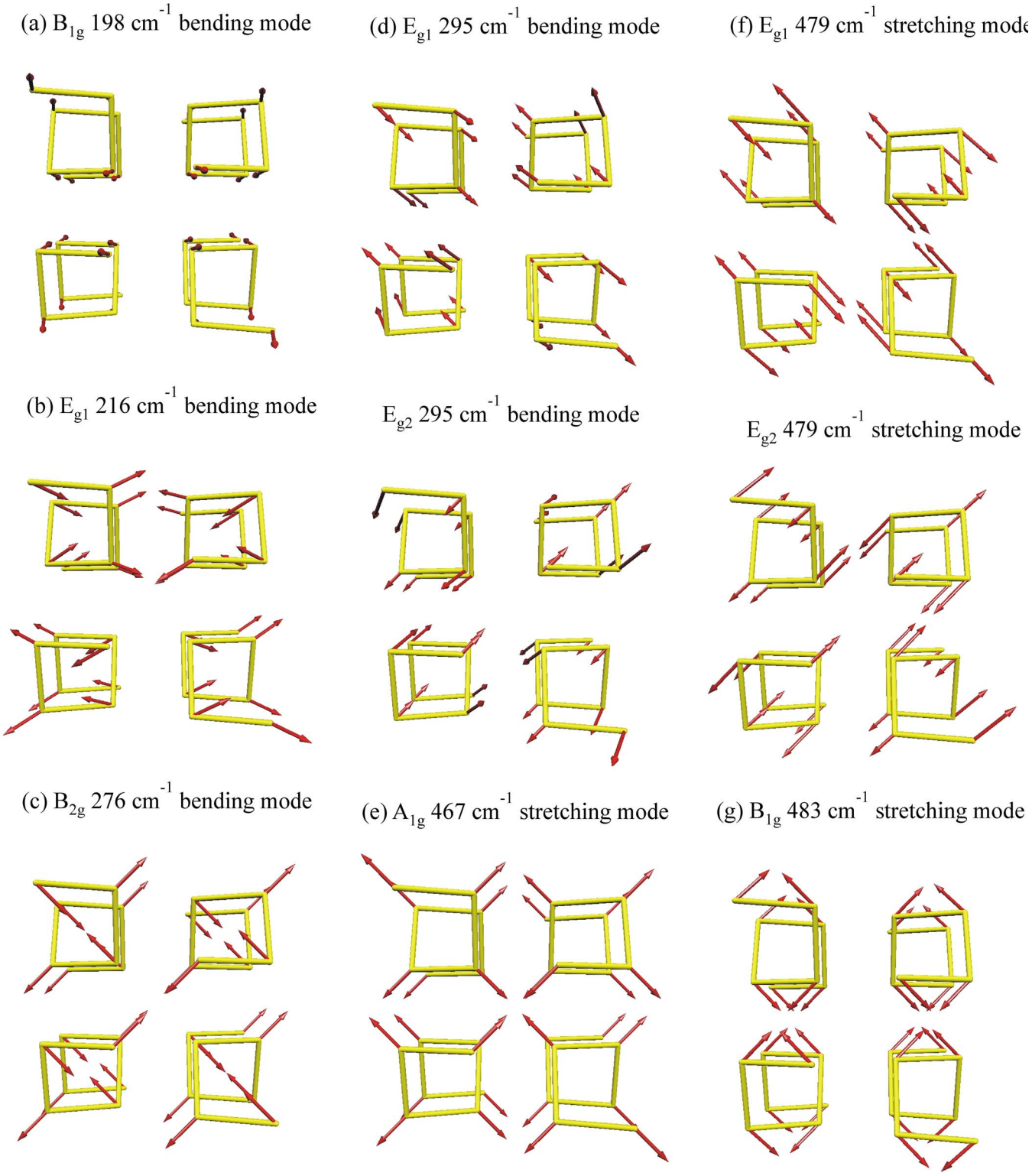

FIG. 9. (Color online) Raman active modes of the S-III phase with the square spiral chain structure, calculated for a pressure of 37 GPa. The 216 cm^{-1} E_{g2} mode is not shown.

the first time. This study has also allowed us to identify a previously observed high-pressure low-temperature phase as S-III.

The sulfur high-pressure phases having polymeric chains of triangular geometry (S-II) and S_6 molecules (S-VI) are observed by x-ray diffraction at high temperatures close to melting, whereas the same phases can be observed at room temperature by Raman spectroscopy with the sample exposed to laser illumination. The higher pressure phase with polymeric chains of square geometry (S-III) observed by x-ray diffraction above 36 GPa at room temperature, and above 11 GPa at high temperatures can be observed by Raman spectroscopy at room temperature at pressures above 12 GPa by using low-power laser. It appears that for all high-

pressure transitions between the chain and ring phases found in sulfur and selenium, the absorption of the laser light in the Raman measurements plays a crucial role in facilitating these transitions. The same phases are observed under pressure by x-ray diffraction if external heating is applied.

ACKNOWLEDGMENTS

The authors thank A. F. Goncharov and V. V. Struzhkin for assistance with Raman scattering experiments and helpful discussions. This work and HPCAT is supported by DOE-BES, DOE-NNSA (CDAC), DOD-TACOM, NSF, NASA, and the W. M. Keck Foundation. The authors acknowledge the financial support from NSF through Grant No. EAR-0217389. The Advanced Photon Source is supported by the U.S. Department of Energy, Office of Science, Office of Basic Energy Sciences under Contract No. W-31-109-Eng-38. One of the authors (E.R.H.) wishes to thank the Spanish Ministry of Science and Education (Grant No. BFM2003-03372-C03) and the Catalan Regional Government (Grant No. 2005SGR683) for funding.

[1] W. A. Crichton, G. B. M. Vaughan, and M. Mezouar, Z. Kristallogr. **216**, 417 (2001).
[2] H. Fujihisa, Y. Akahama, H. Kawamura, H. Yamawaki, M. Sakashita, T. Yamada, K. Honda, and T. Le Bihan, Phys. Rev. B **70**, 134106 (2004).
[3] O. Degtyareva, E. Gregoryanz, M. Somayazulu, P. Dera, H. K. Mao, and R. J. Hemley, Nat. Mater. **4**, 152 (2005).
[4] L. Crapanzano, W. A. Crichton, G. Monaco, R. Bellissent, and M. Mezouar, Nat. Mater. **4**, 550 (2005).
[5] C. Hejny, L. F. Lundegaard, S. Falkoni, M. I. McMahon, and M. Hanfland, Phys. Rev. B **71**, 020101(R) (2005).
[6] O. Degtyareva, E. Gregoryanz, M. Somayazulu, H. K. Mao, and R. J. Hemley, Phys. Rev. B **71**, 214104 (2005).
[7] H. Luo, R. G. Greene, and A. L. Ruoff, Phys. Rev. Lett. **71**, 2943 (1993).
[8] W. Haefner, H. Olijnyk, and A. Wokaun, High Press. Res. **3**, 248 (1990).
[9] W. Haefner, J. Kritzenberger, H. Olijnyk, and A. Wokaun, High Press. Res. **6**, 57 (1990).
[10] P. Wolf, B. Baer, M. Nicol, and H. Cynn, in *Molecular Systems under High Pressure*, edited by R. Pucci and G. Picciotto (Elsevier, Amsterdam, 1991), p. 263.
[11] K. Nagata, T. Nishio, H. Taguchi, and Y. Mihiamoto, Jpn. J. Appl. Phys., Part 1 **31**, 1078 (1992).
[12] P. Rossmanith, W. Haefner, A. Wokaun, and H. Olijnyk, High Press. Res. **11**, 183 (1993).
[13] A. Yoshioka and K. Nagata, J. Phys. Chem. Solids **56**, 581 (1995).
[14] I. Orgzall and B. Lorenz, High Press. Res. **13**, 215 (1995).
[15] B. Eckert, H. J. Jodl, H. O. Albert, and P. Foggi, in *Frontiers of High Pressure Research*, edited by H. D. Hochheimer and R. D. Etters (Plenum, New York, 1992), p. 143.
[16] B. Eckert, R. Schumacher, H. Jodl, and P. Foggi, High Press. Res. **17**, 113 (2000).
[17] A. Anderson, W. Smith, and J. F. Wheeldon, Chem. Phys. Lett. **263**, 133 (1996).
[18] A. F. Goncharov, E. Gregoryanz, V. V. Struzhkin, R. J. Hemley, H. K. Mao, N. Boctor, and E. Huang, in *High Pressure Phenomena*, Proceedings of the International School of Physics "Enrico Fermi," Course CXLVII, edited by R. J. Hemley, G. Chiarotti, M. Bernasconi, and L. Ulivi (IOS, Amsterdam, 2002), p. 297.
[19] G. Kresse and J. Furthmüller, Phys. Rev. B **54**, 11169 (1996); Comput. Mater. Sci. **6**, 15 (1996); G. Kresse and J. Hafner, J. Phys.: Condens. Matter **6**, 8245 (1994).
[20] P. Hohenberg and W. Kohn, Phys. Rev. **136**, 864 (1964); W. Kohn and L. J. Sham, *ibid.* **140**, 1133 (1965).
[21] K. Parlinski, PHONON, 2005.
[22] P. E. Blöchl, Phys. Rev. B **50**, 17953 (1994).
[23] G. Kresse and D. Joubert, Phys. Rev. B **59**, 1758 (1999).
[24] J. P. Perdew, K. Burke, and M. Ernzerhof, Phys. Rev. Lett. **77**, 3865 (1996).
[25] O. Degtyareva, E. Gregoryanz, H. K. Mao, and R. J. Hemley, High Press. Res. **25**, 17 (2005).
[26] M. I. Aroyo, A. Kirov, C. Capillas, J. M. Perez-Mato, and H. Wondratschek, Acta Crystallogr., Sect. A: Found. Crystallogr. **62**, 115 (2006); M. I. Aroyo, J. M. Perez-Mato, C. Capillas, E. Kroumova, S. Ivantchev, G. Madariaga, A. Kirov, and H. Wondratschek, Z. Kristallogr. **221**, 1 (2006).
[27] K. Aoki, O. Shimomura, S. Minomura, N. Koshizuka, and T. Tsushima, J. Phys. Soc. Jpn. **48**, 906 (1980).
[28] R. Schumacher, B. Eckert, and H. J. Jodl, High Press. Res. **15**, 105 (1996).
[29] J. Berkowitz, W. A. Chupka, E. Bromels, and R. L. Belford, J. Chem. Phys. **47**, 4320 (1967).
[30] L. A. Nimon, V. D. Neff, R. E. Cantley, and R. O. Buttlar, J. Mol. Spectrosc. **22**, 105 (1967).
[31] M. W. Wong, Y. Steudel, and R. Steudel, J. Chem. Phys. **121**, 5899 (2004).
[32] A. K. Bandyopadhyay and L. C. Ming, Phys. Rev. B **54**, 12049 (1996).
[33] H. Liu, C. Jin, and Y. Zhao, Physica B **315**, 210 (2002).
[34] C. Hejny and M. I. McMahon, Phys. Rev. Lett. **91**, 215502 (2003).
[35] B. Eckert and R. Steudel, Top. Curr. Chem. **231**, 31 (2003).
[36] R. Steudel and B. Eckert, Top. Curr. Chem. **230**, 1 (2003).
[37] M. I. McMahon, C. Hejny, J. S. Loveday, L. F. Lundegaard, and M. Hanfland, Phys. Rev. B **70**, 054101 (2004).
[38] C. Hejny and M. I. McMahon, Phys. Rev. B **70**, 184109 (2004).
[39] W. B. Holzapfel, T. Krueger, W. Sievers, and V. Vijayakumar, Jpn. J. Appl. Phys., Part 1 **32**, 16 (1993).
[40] J. Steidel, J. Pickardt, and R. Steudel, Z. Naturforsch. B **33**, 1554 (1978).